Published in final edited form as:
Peptides. 2009 May ; 30(5): 866–872. doi:10.1016/j.peptides.2009.01.010.

Non-strict Strand Orientation of the Ca^{2+}-induced Dimerization of a Conantokin Peptide Variant with Sequence-shifted γ-carboxyglutamate Residues

Qiuyun Dai[‡,§], **Cai Xiao**[‡], **Mingxin Dong**[‡], **Zhuguo Liu**, **Zhenyu Sheng**[¶], **Francis J. Castellino**[¶], and **Mary Prorok**[¶,§]

[‡]From Beijing Institute of Biotechnology, Beijing 100071, China

[¶]Department of Chemistry and Biochemistry, University of Notre Dame, Indiana 46556, USA

Abstract

We have previously found a new mode of metal ion–induced helix-helix assembly for the γ-carboxyglutamate (Gla)-containing, neuroactive conantokin (con) peptides that is independent of the hydrophobic effect. In these unique "metallo-zipper" assemblies of con-G and con-T[K7γ], interhelical Ca^{2+} coordination induces dimer formation with strictly antiparallel chain orientation in conantokin peptides in which Gla residues are positioned at "i, i + 4, i +7, i + 11" intervals. In order to probe the property of self-assembly in conantokin peptides with an extended Gla network, a con-T variant (con-T-tri) was synthesized that contains five Gla residues spaced at "i, i + 4, i +7, i + 11, i + 14" intervals. Sedimentation equilibrium analyses showed that Ca^{2+}, but not Mg^{2+}, was capable of promoting con-T-tri self-assembly. Oxidation and rearrangement assays with Cys-containing con-T-tri variants revealed that the peptide strands in the complex can orient in both parallel and antiparallel forms. Stable parallel and antiparallel dimeric forms of con-T-tri were modeled using disulfide-linked peptides and the biological viability of these species was confirmed by electrophysiology. These findings suggest that small changes within the helix-helix interface of the conantokins can be exploited to achieve desired modes of strand alignment.

Keywords

Conantokin peptides; self-association; γ-carboxyglutamic acid; dimerization; strand alignment

1. Introduction

It is generally accepted that protein folding, in naturally-occuring and engineered systems alike, is driven by the hydrophobic effect. Intra- and intermolecular helix-helix assemblies, as found in coiled-coil domains of soluble proteins or in membrane-spanning helical bundles, are prime examples of this precept. In the former case, minimizing the exposure of apolar surface area to the aqueous milieu provides the energetic drive for coiled-coil formation [7,3], whereas

§To whom correspondence should be addressed: Beijing Institute of Biotechnology, Beijing 100071, China. Tel: 86-10-66948897. Fax: 86-10-63833521. Email: E-mail: qy_dai@yahoo.com.cn. §To whom correspondence should be addressed: Department of Chemistry and Biochemistry, University of Notre Dame, Indiana 46556, USA. Tel.: 574-6319120. Fax: 574-6314048. Email: E-mail: mprorok@nd.edu.

maximizing contacts between lipophilic side-chains and the hydrocarbon core of the bilayer directs protein folding in the membrane [20]. Hence, in aqueous solution, the interface of interacting amphipathic helices is defined by hydrophobic residues, whereas polar and charged residues reside on the outer face of the complex. The opposite arrangement prevails for amphipathic helix assemblies in the membrane bilayer.

Recently, we have identified two, γ-carboxyglutamate (Gla)-rich neuroactive peptides that, in the presence of Ca^{2+}, dimerize in a novel manner [9,10,11,6]. One of these, conantokin (con)-G (GE γγLQγNQγLIRγKSN-NH_2) is a naturally–occurring peptide found in the venom of the predatory snail *Conus geographos*. The other is a variant of a conantokin (con-T) derived from *Conus tulipa* and differs from the parent peptide by virtue of a Lys to Gla replacement at sequence postion 7 (con-T[K7γ]; GEγγYQγMLγNLRγAEVKKNA-NH_2). Both peptides are potent and specific inhibitors if ion flow through N-methyl-D-aspartate (NMDA) receptor complexes. Both con-G and con-T[K7γ] are maintained in the dimeric state through interhelical Ca^{2+}-Gla coordination within the helix interface, while hydrophobic and uncharged amino acids line the outer faces of the dimer. This unique "metallo-zipper" dimer motif is contingent upon optimal spacing of the Gla network within each peptide, specifically an *"i, i + 4, i +7, i + 11"* arrangement of Gla residues. In addition to the purely electrostatic interactions that stabilize the interhelical core, conantokin dimers are also typified by an antiparallel orientation of their constituent peptide strands. These findings have import in the realm of protein design, wherein the precise, yet reversible, folding of secondary structural elements is desired. In order to test the effect of extending the Gla network in a dimerizing conantokin, we synthesized and characterized a triple con-T variant, con-T[γ4E,K7γ,V17γ] (con-T-tri), that contains an *"i, i + 4, i + 7, i + 11, i +14"* distribution of Gla. The effects of this sequence alteration on the dimerization tendency and strand alignment of the peptide are reported herein.

2. Materials and Methods

2.1. Peptide Synthesis, purification, and characterization

The peptides employed in this study, which are depicted in Fig. 1, were synthesized, purified, and characterized as previously described [22]. All Fmoc-derivatized amino acids were obtained from either Sigma (St. Louis, MO) or Novabiochem (San Diego, CA) with the exception of Fmoc-γ,γ'-di-o-tBu-L-Gla, which was synthesized as reported earlier [8]. Procedures for obtaining the disulfide-linked peptides used in thiol-disulfide rearrangement assays were similar to those previously described [9].

2.2. Determination of Peptide Strand Orientation

Strand orientation preference was determined through thiol-disulfide oxidation and rearrangement experiments, as previously outlined [9]. For the oxidation experiments, a 1:1 molar ratio of C^0-con-T-tri and C^{21}-con-T-tri, at a concentration of 400 μM each, were stirred in an open vial at room temperature in a total volume of 0.35 mL of folding buffer (50 mM sodim borate/100 mM NaCl, pH 8.2). The progress of the oxidation was monitored by analytical reverse-phase HPLC as follows: 30 μl of the reacting solution was injected onto an HPLC column (Kromasil C_{18}, 4.6mm × 250 mm) equilibrated in 90:10 (v:v) 0.1% TFA:0.1 % TFA/CH_3CN at a flow rate of 1.0 ml/min. At 1 min post-injection, a 40 min linear gradient was applied to a limiting value of 55:45 (v:v) 0.1% TFA:0.1% TFA/CH_3CN. Absorbance detection was performed at 220 nm. Individual peaks were collected, lyophilized and characterized by DE-MALDI-TOF-MS.

In the thiol-disulfide rearrangement experiments, the homomeric disulfide-linked peptides, di-C^0-con-T-tri and di-C^{21}-con-T-tri, were separately dissolved in 50 mM sodium borate/100 mM NaCl, pH 8.2, at a concentration of 200 μM. An aliquot of reduced C^{21}-con-T-tri was added

to the di-C^0-con-T-tri solution, while an aliquot of reduced C^0-con-T-tri was added to the di-C^{21}-con-T-tri solution. $CaCl_2$ was added to a final concentration of 20 mM. In both cases the initial reduced monomer/dimer molar ratio was 2:1 and the reactions were maintained under a blanket of N_2. Aliquots were removed at selected intervals and analyzed by analytical reverse-phase HPLC using the procedure detailed in the previous paragraph.

2.3. Circular dichroism spectroscopy

CD spectra were recorded between 195 nm and 260 nm on a Jasco J-715 spectropolarimeter as described earlier [9]. The helical content of each peptide was determined from the relationship, $\text{fraction}_{\text{helix}} = (-[\Theta]_{222} - 2340)/30{,}300$ [5].

2.4. Isothermal titration calorimetry

The binding isotherms of metal ions to con-T-tri was determined at 25 °C with a MicroCal (Northampton, MA) VP-ITC microcalorimeter in a buffer consisting of 10 mM Na-MES/100 mM NaCl, pH 6.5. Peptide samples ranging in concentration from 0.3–0.5 mM were introduced into the reaction cell. Injections (3–5 μl) of either 100 mM $CaCl_2$ or 50 mM $MgCl_2$, in matching Na-MES buffer, were delivered at discrete intervals. The data was corrected for heat of dilution of the metal ion solution by performing a matching titration of metal ion into buffer in the absence of peptide. The titration curves were deconvoluted for the best-fit model using the ORIGIN for ITC software package supplied by MicroCal.

2.5. Analytical ultracentrifugation

Sedimentation equilibrium experiments were performed using an Optima XL-I analytical ultracentrifuge (Beckman Instruments, Palo Alto, CA) in an An-60 Ti rotor equipped with a standard two-channel cell. Peptides were dissolved in 10 mM sodium borate/100 mM NaCl buffer, pH 6.5, at a concentration of 150 μM. The peptide samples in the absence and presence of metal ion were independently rotated at speeds 32,000, 45,000 and 52,000 rpm at 20° C until equilibrium was attained. Absorbance monitoring was performed at 230 nm or 280 nm. For each peptide, 2 or 3 separate sedimentation equilibrium analyses were performed. The apparent molecular weight (MW_{app}) was obtained by global fitting of multiple scans acquired at 45,000 and 52,000 rpm (3–5 scans at each speed) to a single ideal species using the sedimentation analysis software supplied by Beckman. The partial specific volumes assigned to con-T-tri, di-C^0-con-T-tri, di-C^0-con-T-tri, and C^0/C^{21}-con-T-tri were 0.705, 0.702, 0.701, and 0.702 mL/g, respectively, as calculated from the mass average of the partial specific volumes of the individual amino acids [16]. Gla residues were assigned the partial specific volume value of glutamate (0.66 mL/g). The fractional dimer content of self-associating peptides at equilibrium was calculated as previously described [9] and is based on the precept that the sum of fractional dimer and monomer contents is unity.

2.6. Electrophysiology

Whole-cell patch clamp recordings were conducted on HEK293 cells transiently expressing combinations of NR1b and NR2 (A or B) NMDA receptors as detailed in a prior study [15]. Cells were maintained at a holding potential of −70 mV. The extracellular solution consisted of 140 mM NaCl, 3 mM KCl, 2 mM $CaCl_2$, 10 mM Na-Hepes, and 20 mM dextrose, pH 7.35. Recording pipettes contained 140 mM CsF, 1 mM $CaCl_2$, 2 mM $MgCl_2$, 10 mM EGTA, 10 mM Cs-Hepes, 2 mM tetraethylammonium chloride, and 4 mM Na_2ATP, pH 7.35. Currents were evoked with the application of extracellular solution containing100 μM NMDA and 10 μM glycine. Con-T-tri and disulfide-linked variants of con-T-tri were applied at a concentration of 40 μM. Solutions were applied using a nine-barrel rapid solution changer (Biologic, Calix, France) positioned 200–300 μM from the cell being perfused. Data were filtered at 5 kHz,

digitized and acquired on a personal computer using pClamp software (Axon Instruments, Foster City, CA).

3. Results

3.1. Ca^{2+} induced self-assembly in peptides with an extended Gla network

In order to determine the extent of self-association in a con-T derivative with a Gla distribution of "i, i + 4, i +7, i + 11, i + 14", the Gla residue at sequence position 4 of con-T was replaced by Glu while Lys7 and Val17 were both replaced by Gla. As determined by CD spectroscopy, con-T-tri, like the con-T[K7γ] parent peptide, displays marginal helicity in the absence of divalent metal ions, but assumes a high percentage of helix content in the presence of saturating Ca^{2+} and Mg^{2+} (Table 1, Fig. 2). The affinities and stoichiometries for Ca^{2+} and Mg^{2+} binding to this peptide were ascertained by isothermal titration calorimetry (ITC). As shown in Fig. 3 and summarized in Table 1, incremental additions of $CaCl_2$ or $MgCl_2$ into con-T-tri resulted in exothermic heat changes that, following deconvolution, revealed two distinct classes of binding sites ($n_1 = 2.2$, $n_2 = 6.4$) for Ca^{2+} and a single site ($n = 1.0$) for Mg^{2+}. The K_d values obtained for Ca^{2+} binding to the first and second classes of sites were 26 μM and 344 μM, respectively, whereas Mg^{2+} binding was characterized by a K_d value of 125 μM. These results indicate that the binding mode of Ca^{2+} to con-T-tri is different from that of Mg^{2+}. Furthermore, when comparing these con-T-tri values to the Ca^{2+} and Mg^{2+} stoichiometries and binding constants previously obtained for con-T[K7γ] (Table 1, [10]), it is apparent that the mode of metal ion binding differs considerably between the two peptides.

The sedimentation equilibrium results for the resultant peptide, con-T-tri, in the absence and presence of Ca^{2+} ions are shown in Fig. 4 and summarized in Table 1. In the apo form, con-T-tri exhibited a monomeric MW_{app} of 3320, which is within 20% of the calculated sequence-based MW of 2760. In the presence of 20 mM Ca^{2+}, this value is increased to 6490. When taking a bound Ca^{2+} stoichiometry of 8 into account (*vide supra*), the MW_{app} of the Ca^{2+}-associated peptide is consistent with a fractional dimer content of 0.76. In contrast to Ca^{2+}, addition of 20 mM Mg^{2+} to apo con-T-tri did not result in marked self-association. These results are consonant with those observed for con-T[K7γ] [10] and indicate that including an additional Gla residue to yield *i, i + 4, i +7, i + 11, i + 14* spacing promotes dimerization to an extent similar to that obtained for an "*i, i + 4, i +7, i + 11*" distribution of Gla residues. The MW_{app} values for the disulfide-linked Cys-containing homo- and heterostranded peptides were also obtained by sedimentation equilibrium and are included in Table 1. In the presence of Ca^{2+}, di-C^{21}-con-T-tri and C^0/C^{21}-con-T-tri display a very slight tendency to form higher order assemblies, whereas a higher order structure predominates for Ca^{2+}-complexed di-C^0-con-T-tri.

3.2. Relative peptide chain orientation of self-associating con-T-tri

Thiol-disulfide oxidation and rearrangement assays with Cys-containing peptides are frequently used to determine the relative strand orientation of helical dimers and higher order peptide assemblies [14,18,2]. We have previously used this technique to determine the alignment preferences of con-G/Ca^{2+} and con-T[K7γ]/Ca^{2+} homodimers, as well as the heterodimeric Ca^{2+}-mediated complex between con-G and con-T[K7γ] [9,10,11]. In all three systems, a strong tendency for an antiparallel alignment of peptide chains was observed. The validity of the results obtained through this indirect biochemical approach were later confirmed through crystallographic analysis of con-G/Ca^{2+} and con-T[K7γ]/Ca^{2+} dimer complexes [6]. In the present study, the preference for relative helix orientation in the con-T-tri dimer was assessed by evaluating the oxidation products formed between two Cys-containing con-T-tri variants, C^0-con-T-tri and C^{21}-con-T-tri. Because our initial model of the con-T-tri/Ca^{2+} dimer (based on that of con-G/Ca^{2+} and con-T[K7γ]/Ca^{2+}) consisted of a Gla core (designated as

positions *a* and *d* in the heptad template) involving Gla residues 3, 7, 10, 14 and 17, the placement of Cys in each variant also occurs at positions *a* or *d* in the heptad repeat (Fig. 1). The equilibrium distribution of products resulting from co-incubation of C^0-con-T-tri and C^{21}-con-T-tri in the absence and presence of Ca^{2+} and Mg^{2+} is shown in the series of chromatograms in Fig. 5. The distribution of oxidized products differs only slightly among metal ion-free, Ca^{2+}-containing, and Mg^{2+}-containing buffer conditions. Only a small excess of the heterostranded, antiparallel product, C^0/C^{21}-con-T-tri, prevails over the parallel-oriented di-C^{21}-con-T-tri homomer at equilibrium in all three buffers. This is in contrast to the product profile of the analogous Cys-containing versions of con-G and con-T[K7γ] that were observed in previously conducted studies [9,10]. In these studies, the antiparallel disulfide products predominated in Ca^{2+}-containing buffer, while all three possible products were observed in metal-ion free and Mg^{2+}-containing buffers. These results suggest that the con-T-tri/Ca^{2+} dimer can exist in both parallel and antiparallel strand orientations.

The nonspecific strand orientation was also supported by the results of related experiments in which the N- and C-linked homodimers, di-C^0-con-T-tri and di-C^{21}-con-T-tri, were individually incubated with C^0-con-T-tri and C^{21}-con-T-tri in Ca^{2+}-containing buffer. As shown in Fig. 6, when beginning with C^0-con-T-tri and di-C^{21}-con-T-tri in a 2:1 molar ratio (trace a), at equilibrium, the heteromeric disulfide product was in just slight excess of the homodimer, di-C^{21}-con-T-tri (trace b). In the complement experiment, in which di-C^0-con-T-tri and C^{21}-con-T-tri were the initial reactants, an equal distribution of hetero- and homostranded (mainly di-C^{21}-con-T-tri) disulfide-linked peptides were observed (traces c, d). These results reinforce the notion that in the presence of Ca^{2+}, con-T-tri can self-associate in parallel and antiparallel motifs alike.

3.3 The NMDAR activity of con-T-tri and disulfide-constrained con-T-tri variants

The con-T-tri peptide described in this study is based on the naturally-occurring conantokin, con-T (Fig. 1), a potent and selective inhibitor of current flow through the NMDA receptor [13]. Functional NMDA receptors require the coassembly of two subunit families, NR1 and NR2. In the brain, the subtypes of NR1 and NR2 that predominate are 1a and 1b, and 2A and 2B, respectively. Whole cell voltage clamp experiments performed on HEK293 cells transfected with specific combinations of NR1a/b and NR2A/B subunits reveal that con-T exerts similar inhibitory potency at NR1a/NR2A-, NR1a/NR2B-, NR1b/NR2A-, and NR1b/NR2B-containing receptors [25]. In contrast, con-G, a conantokin peptide bearing high sequence homology to con-T, selectively inhibits NR2B-containing receptors and is inactive at NR2A-expressing combinations [15,12]. However, subtle manipulations of the primary sequences of either conantokin can affect the selectivity characteristics of these peptides. For instance, replacement of Leu5 in con-G with Tyr (the amino acid that resides at position 5 in con-T) confers broad NMDA receptor selectivity on the resulting con-G–based peptide, whereas Ala or Gln replacements for Met8 in con-T abolish inhibitory activity at NR2A-containing receptors [15,25]. With these consequences in mind, we opted to use electrophysiology to evaluate the NMDA receptor activity of con-T-tri, a triple variant of con-T. Also, because the low concentrations of Ca^{2+} in the physiological milieu would result in an equilibrium mixture of monomeric and dimeric con-T-tri species, confounding the interpretation of electrophysiology data, the disulfide-constrained parallel and anti-parallel versions of con-T-tri were tested as models of the noncovalent dimeric forms. The two subunit combinations examined were NR1b/2A and NR1b/2B. A single peptide concentration of 40 μM was employed for all experiments—a concentration at which con-T completely antagonizes NMDA receptor activity at all subunit combinations [25]. None of the four peptides tested were able to antagonize NMDA-evoked current at NR1b/2A-expressing cells, although application of con-T-tri and di-C^{21}-con-T-tri resulted in current potentiation at these receptors. In cells transfected with the NR1b/2B subunit combination, con-T-tri, di-C^{21}-con-T-tri, and

C^0/C^{21}-con-T-tri showed modest inhibitory activity. The C-terminally linked disulfide, di-C^0-con-T-tri, was without effect in both expressors.

4. Discussion

In previous work, we have shown that conantokin peptides with an "i, i + 4, i + 7, i + 11" spacing of Gla residues can form antiparallel dimers in the presence of Ca^{2+}. [9,10,11,6]. The physiological significance of the antiparallel-aligned dimer was demonstrated in studies in which a disulfide-constrained antiparallel form of con-G was found to inhibit NMDA receptor activity, whereas the parallel version was without effect [11]. In the present study, we have examined the effect of extending the Gla network in one of these peptides, con-T[K7γ], on dimerization and strand alignment tendencies. This extension was carried out by replacing Val17 in con-T[K7γ] with a Gla residue. Additionally, Gla4 of the parent peptide was replaced by a Glu residue, as prior biochemical and structural data have shown that Gla4 does not participate in Gla-Ca^{2+}-Gla intermolecular bridging interactions within the dimer core [9,10, 11,6]. This replacement therefore insures that the characteristics of the resultant peptide can be unambiguously ascribed to an "i, i + 4, i + 7, i + 11, i + 14" pattern of Gla spacings. The resulting peptide, con-T-tri, displayed negligible helicity in the absence of metal ions, but adopted highly helical character in the presence of Ca^{2+} and Mg^{2+}. The degree of helicity induced by the addition of saturating levels of Ca^{2+} or Mg^{2+} is similar to that observed with con-T[K7γ], indicating that the amino acid changes introduced into con-T-tri do not alter the secondary structure of the peptide relative to con-T[K7γ]. Also consonant with con-T[K7γ] is the ability of con-T-tri to undergo Ca^{2+}- but not Mg^{2+}-mediated dimerization. The same metal ion selectivity, with respect to triggering dimerization, has also been established for con-G [9], despite the fact that Mg^{2+} binds con-G with at least 10-fold higher affinity than Ca^{2+}[21] and promotes the CD-monitored helix formation of con-G at an EC_{50} of 0.12 mM, compared with a value of 3.9 mM obtained for Ca^{2+} [1]. An explanation for the inability of Mg^{2+} to induce dimerization in these peptides can be posited from examination of the crystal structures of the Ca^{2+}-complexed con-T[K7γ] and con-G dimers. These structures reveal that both inter- and intrahelical Ca^{2+} binding to the carboxylate groups of Gla residues are characterized by high Ca^{2+} coordination numbers and irregular coordination geometries. Mg^{2+}, on the other hand, is usually octahedrally coordinated and would not be expected to be able reproduce the coordination modes adopted by Ca^{2+}. Additionally, the smaller ionic radius of Mg^{2+} (145 pm) compared with Ca^{2+} (194 pm) would make Mg^{2+} less likely to effectively bridge the interhelical distances that exist in the Ca^{2+}-complex.

The fractional dimer contents of Ca^{2+}-complexed con-T[K7γ] and con-T-tri were similar (*ca*. 0.75) and, given the initial concentrations of 150 μM employed for each peptide during the sedimentation experiments, correspond to monomer-dimer equilibrium constants of approximately 20 μM. However, despite the similarities in Ca^{2+}-induced helix and fractional dimer content between con-T-tri and con-T[K7γ], the ITC data suggests that the mode of Ca^{2+} binding is very different between the two peptides. Whereas con-T[K7γ] possesses a single class of Ca^{2+} binding site with an occupancy of 3 mol Ca^{2+} per mol monomeric peptide (6 mol Ca^{2+} per mol dimer), con-T-tri contains two classes of Ca^{2+} sites: a high affinity site with an *n* of 2, and a lower affinity site with a stoichiometry of approximately 6. It is not clear if these additional sites are participating in interhelical coordination, but it is reasonable to expect that additional interhelical Ca^{2+} bridging interactions would lead to an increase in helix-helix affinity. As this is not the case, based on the extent of dimerization observed for the two peptides, the Val17Gla and the Gla4Glu replacements in con-T-tri may distort the helix backbone and alter the disposition of side chains relative to con-T[K7γ], resulting in the creation of intrahelical Ca^{2+} sites.

The observation that the equilibrium distribution of disulfide-bridged con-T-tri variants does not reflect a strong preference for antiparallel peptide chain orientation suggests that the interface of the con-T-tri dimer is significantly different from that found for con-T[K7γ]. This is not surprising in light of the results of recent x-ray crystallographic analyses of con-G and con-T[K7γ] [6]. Despite sharing sequence identity at nine sequence positions (including the five Gla positions) and an antiparallel mode of strand orientation, the interhelical cores of the crystallized dimer forms of the two peptides are strikingly different. For instance, three Ca^{2+} are present in the dimer interface of con-G, whereas con-T[K7γ] has four Ca^{2+}. The con-T [K7γ] structure also contains a spine of six water molecules that span the length of the Ca^{2+} network, a feature that is not found in the con-G structure. The helix-helix axial alignments also differ between the two structures, with the two helices of con-T[K7γ] nearly parallel, while those of con-G are skewed out of plane by approximately 30°. Additionally, the side chain of Gln6, which occupies position *g* in the helical heptad repeat, inserts directly into the interface in dimeric con-G, but is flipped away from the interface in dimeric con-T[K7γ]. Although these structural differences between con-G and con-T[K7γ] do not alter the strand alignment orientation of the dimer, they serve to underscore the contribution that residues outside of the Gla core can make towards the structure of the complex. Numerous examples populate the literature indicating that subtle changes in core (*a* and *d* or *g* and *e*) residues can reverse the orientation and/or alter the stoichiometry of oligomerization [18,19,17,24,26].

A noteworthy feature of the Cys-containing peptide oxidation and thiol-disulfide exchange studies concerns the higher stability of the C-terminally linked disulfide peptide, di-C^{21}-con-T-tri compared with the N-terminal species, di-C^{0}-con-T-tri, even though both peptides were designed to provide for disulfide linkages between *a-a* heptad positions within the dimer interface. Not only does di-C^{21}-con-T-tri prevail in the exchange experiments in which C^{0}-con-T-tri and di-C^{21}-con-T-tri are the initial reactants, but it also predominates in the converse experiment. The sedimentation equilibrium data reveal that, in the presence of Ca^{2+}, di-C^{21}-con-T-tri has no tendency to form a higher order species whereas the N-terminally-linked species, di-C^{0}-con-T-tri, assumes a high degree (f_{di} = 0.66) of Ca^{2+}-induced dimer content. These results indicate that the peptide strands of di-C^{21}-con-T-tri can engage in stable, intramolecular Ca^{2+}-bridging that is more refractory to thiol-disulfide exchange than di-C^{0}-con-T-tri, for which intermolecular contacts appear to dominate. The mode of dimerization assumed by di-C^{0}-con-T-tri (parallel, antiparallel or a mixture) cannot be deduced from these studies. The different folding outcomes for di-C^{0}-con-T-tri and di-C^{21}-con-T-tri reinforce the suggestion that minor variations in sequence can be exploited to direct intra- versus intermolecular associations in appropriately designed peptides.

Lastly, the biological activity of con-T-tri in monomeric and the disulfide-constrained parallel and anti-parallel dimeric forms was examined by whole-cell patch clamping of HEK293 cells transfected with NR1b/2A and NR1b/2B subunit combinations. These results demonstrate that with respect to NR2A- and NR2B-selectivity, at least one of the three substitutions in con-T that afford con-T-tri, *viz*., γ4→E, K7→γ and V17→γ, change the inhibitory selectivity of the resultant derivative from non-selective to NR2B selective. Furthermore, at least one of these amino acid replacements confers potentiation of NMDA-evoked responses at NR2A-containing receptors. In a previous study, we have noted a similar activity profile (potentiating at NR2A; inhibiting at NR2B) in a con-T variant containing a M8→Q replacement [25]. However, other Met8-substituted peptides, including con-T[M8N], retain the non-selective nature of the con-T parent. Because atomic-level structural information on the con-T/NMDA receptor complex does not exist, it is difficult to rationalize the selectivity switches accompany subtle changes in the con-T primary sequence. Potentiation of currents in NR1b/2A by con-T-tri may reflect occupancy of a second, stimulatory conantokin site on the NMDA receptor [23]. With respect to the constrained dimeric derivatives of con-T-tri, the C-terminally disulfide-linked peptide, di-C^{21}-con-T-tri, mimics the selectivity pattern of monomeric con-

T-tri. This result suggests that the dimerization of con-T-tri, in parallel orientation, does not result in altered NMDA receptor activity. On the other hand, the complete lack of receptor activity associated with di-C^0-con-T-tri is not surprising, as it has been demonstrated that either acetylation of the conantokin N-terminus or introduction of an amino acid N-terminal to Gly1 eliminates the NMDA receptor activity [27,4]. The deleterious effect of modifications to the N-terminus of Gly1 is also reflected in C^0/C^{21}-con-T-tri, the peptide that models the Ca^{2+}-mediated self-association of con-T-tri in antiparallel format. This species exhibits inhibitory activity at NR2B-containing receptors that is intermediate of that seen with C- and N-terminally-linked parallel dipeptides.

5. Conclusions

The results presented herein show that by extending the Gla network within the con-T[K7γ] scaffold, strand alignment following Ca^{2+}-induced dimerization of this peptide switches from strictly antiparallel to a mixture of parallel and antiparallel orientations. Using covalently-constrained models of the parallel and antiparallel dimers forms, we demonstrate that NMDA receptor activity is associated with both orientations. Furthermore, Ca^{2+}-Gla bridging in the homomeric disulfide-linked versions of con-T-tri can occur either intra- or intermolecularly, depending on the location of the disulfide bridge. Overall, these results suggest that as more knowledge of the interactions that direct folding in Gla-containing peptides is acquired, Ca^{2+}-mediated Gla interactions can be utilized to design peptide dimers with specific features, including either parallel or antiparallel chain alignment, and inter- or intramolecular helix-helix contacts.

Acknowledgements

This work was supported by the China Natural Science Foundation (No. 30672446, 90713028, to Q.Y.D.), grant 2006AA09Z404 from the High Technology Program of Oceans in China (to Q.Y.D.), and National Institutes of Health grant HL019982 (to F.J.C.).

References

1. Blandl T, Zajicek J, Prorok M, Castellino FJ. Metal-ion-binding properties of synthetic conantokin-G. Biochem J 1997;328:777–783. [PubMed: 9396720]
2. Burkhard P, Ivaninskii S, Lustig A. Improving coiled-coil stability by optimizing ionic interactions. J Mol Biol 2002;318:901–910. [PubMed: 12054832]
3. Burkhard P, Stetefeld J, Strelkov SV. Coiled coils: a highly versatile protein folding motif. Trends Cell Biol 2001;11:82–88. [PubMed: 11166216]
4. Chandler P, Pennington M, Maccecchini ML, Nashed NT, Skolnick P. Polyamine-like actions of peptides derived from conantokin-G, an N-methyl-D-aspartate (NMDA) antagonist. J Biol Chem 1993;268:17173–17178. [PubMed: 8349604]
5. Chen Y-H, Yang JT, Martinez HM. Determination of the secondary structures of proteins by circular dichroism and optical rotatory dispersion. Biochemistry 1972;11:4120–4131. [PubMed: 4343790]
6. Cnudde SE, Prorok M, Dai Q, Castellino FJ, Geiger JH. The crystal structures of the calcium-bound con-G and con-T[K7γ] dimeric peptides demonstrate a novel metal-dependent helix-forming motif. J Am Chem Soc 2007;129:1586–1593. [PubMed: 17243678]
7. Cohen C, Parry DA. Alpha-helical coiled coils: more facts and better predictions. Science 1994;263:488–489. [PubMed: 8290957]
8. Colpitts TL, Castellino FJ. Binding of calcium to synthetic peptides containing gamma-carboxyglutamic acid. Int J Peptide and Protein Res 1993;41:567–575. [PubMed: 8349415]
9. Dai Q, Prorok M, Castellino FJ. A new mechanism for metal ion-assisted interchain helix assembly in a naturally-occurring peptide mediated by optimally spaced gamma-carboxyglutamic acid residues. J Mol Biol 2004;336:731–744. [PubMed: 15095984]

10. Dai Q, Castellino FJ, Prorok M. A single amino acid replacement results in the Ca^{2+}-induced self-assembly of a helical conantokin-based peptide. Biochemistry 2004;43:13225–13232. [PubMed: 15476416]
11. Dai Q, Sheng Z, Geiger JH, Castellino FJ, Prorok M. Helix-helix interactions between homo- and heterodimeric γ-carboxyglutamate-containing conantokin peptides and their derivatives. J Biol Chem 2007;282:12641–12649. [PubMed: 17347154]
12. Donevan SD, McCabe RT. Conantokin G is an NR2B-selective competitive antagonist of N-methyl-D-aspartate receptors. Mol Pharmacol 2000;58:614–623. [PubMed: 10953056]
13. Haack JA, Rivier J, Parks TN, Mena EE, Cruz LJ, Olivera BM, Conantokin T. A gamma-carboxyglutamate containing peptide with N-methyl-d-aspartate antagonist activity. J Biol Chem 1990;265:6025–6029. [PubMed: 2180939]
14. Harbury PB, Zhang T, Kim PS, Alber T. A switch between two-, three-, and four-stranded coiled coils in GCN4 leucine zipper mutants. Science 1993;262:1401–1407. [PubMed: 8248779]
15. Klein RC, Prorok M, Galdzicki Z, Castellino FJ. The amino acid residue at sequence position 5 in the conantokin peptides partially governs subunit-selective antagonism of recombinant N-methyl-D-aspartate receptors. J Biol Chem 2001:26860–26867. [PubMed: 11335724]
16. Laue, TM.; Shah, BD.; Ridgeway, TM.; Pelletier, SM. Computer-aided interpretation of analytical sedimentation data for proteins. In: Harding, SE.; Rowe, AJ.; Horton, JC., editors. Analytical ultracentrifugation in biochemistry and polymer science. Cambridge: The Royal Society of Chemistry; 1992. p. 90-125.
17. Monera OD, Kay CM, Hodges RS. Electrostatic interactions control the parallel and antiparallel orientation of α-helical chains in two-stranded α-helical coiled-coils. Biochemistry 2001;33:3862–3871. [PubMed: 8142389]
18. Monera OD, Zhou NE, Kay CM, Hodges RS. Comparison of antiparallel and parallel two-stranded alpha-helical coiled-coils. Design, synthesis, and characterization. J Biol Chem 1993;268:19218–19227. [PubMed: 8366074]
19. Oakley M, Kim PS. A buried polar interaction can direct the relative orientation of helices in a coiled coil. Biochemistry 1998;37:12603–12610. [PubMed: 9730833]
20. Popot J-L, Engelman DM. Helical membrane protein folding, stability, and evolution. Ann Rev Biochem 2000;69:881–922. [PubMed: 10966478]
21. Prorok M, Castellino FJ. Thermodynamics of binding of calcium, magnesium, and zinc to the N-methyl-D-aspartate receptor ion channel peptidic inhibitors, conantokin-G and conantokin-T. J Biol Chem 1998;273:19573–19578. [PubMed: 9677382]
22. Prorok M, Warder SE, Blandl T, Castellino FJ. Calcium binding properties of synthetic gamma-carboxyglutamic acid-containing marine cone snail "sleeper" peptides, conantokin-G and conantokin-T. Biochemistry 1996;35:16528–16534. [PubMed: 8987986]
23. Ragnarsson L, Yasuda T, Lewis RJ, Dodd PR, Adams DJ. NMDA receptor subunit-dependent modulation by conantokin-G and Ala7-conantokin-G. J Neurochem 2006;96:283–291. [PubMed: 16336218]
24. Schnarr NA, Kennan AJ. Strand orientation by steric matching: a designed antiparallel coiled-coil trimer. J Am Chem Soc 2004;126:14447–14451. [PubMed: 15521764]
25. Sheng Z, Dai Q, Prorok M, Castellino FJ. Subtype-selective antagonism of N-methyl-D-aspartate receptor ion channels by synthetic conantokin peptides. Neuropharmacology 2007;53:145–156. [PubMed: 17588620]
26. Taylor CM, Keating AE. Orientation and oligomerization specificity of the Bcr coiled-coil oligomerization domain. Biochemistry 2005;44:16246–16256. [PubMed: 16331985]
27. Warder SE, Blandl T, Klein RC, Castellino FJ, Prorok M. Amino acid determinants for NMDA receptor inhibition by conantokin-T. J Neurochem 2001;77:812–822. [PubMed: 11331410]

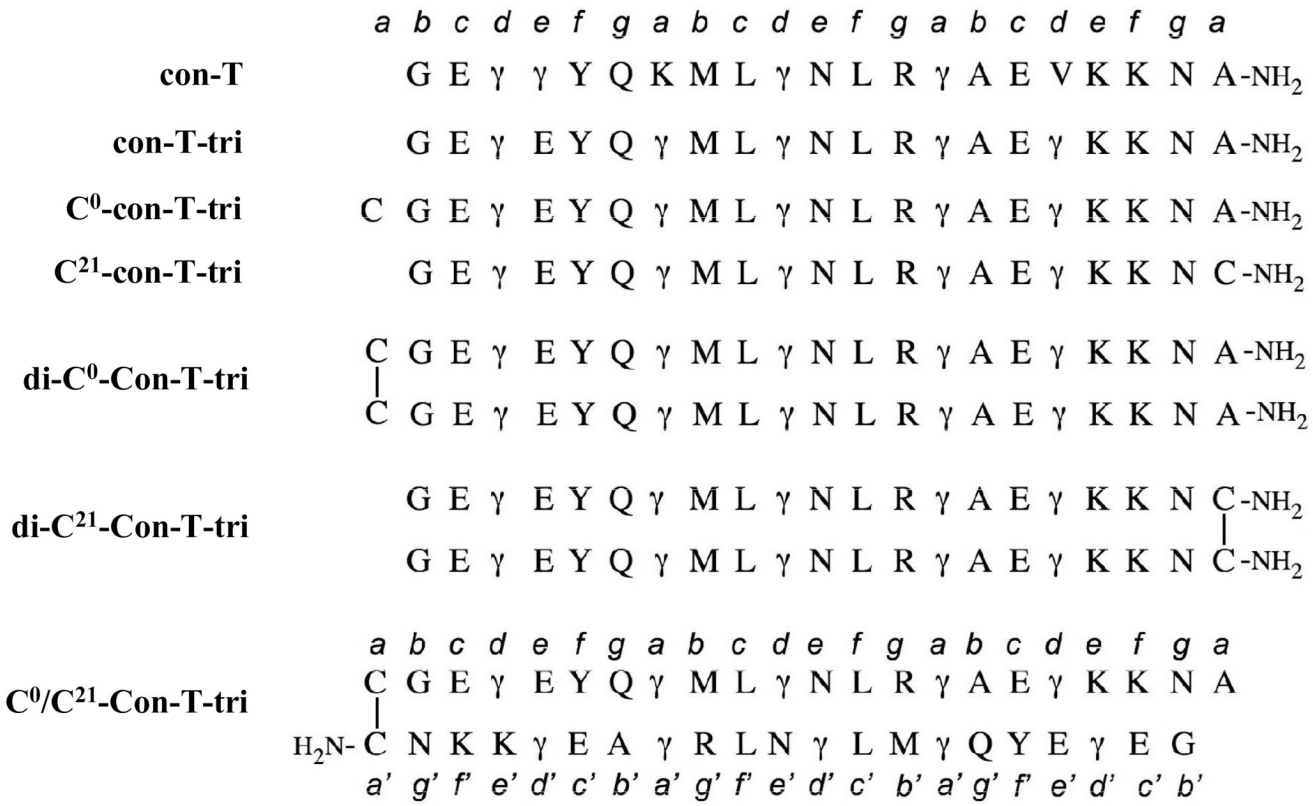

Fig. 1.

Primary sequences of con-T variants in the study. The helical heptad repeat for each peptide is denoted a-g and a'–g'(for antiparallel strands).

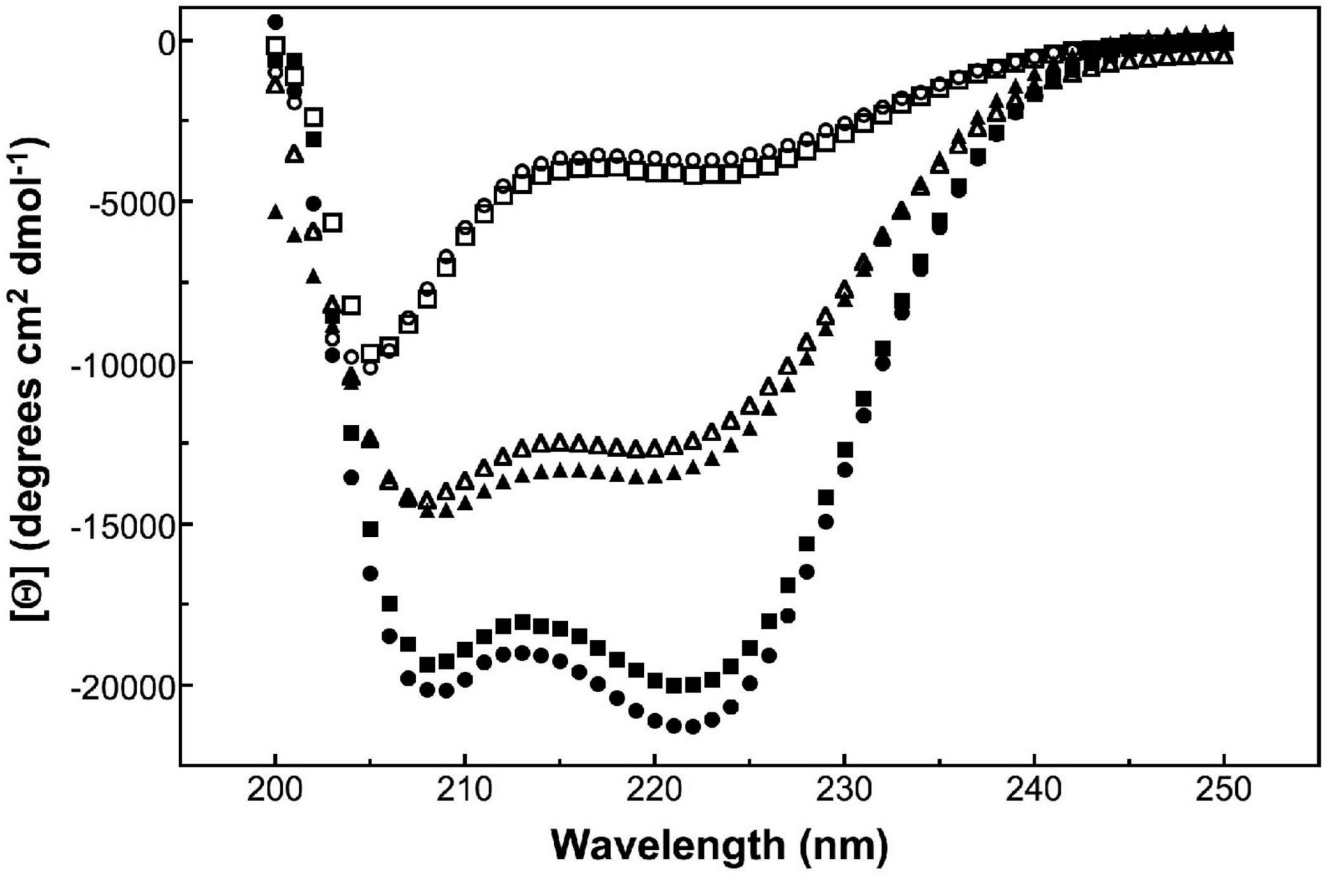

Fig. 2.

CD spectra of con-T-tri and disulfide-linked derivatives in apo form and the presence of Ca^{2+}. Spectra were recorded at 25° C in 10 mM sodium borate/100 mM NaCl, pH 6.5 using a 1.0 cm pathlength cell. (○) con-T-tri; (□) di-C^0-con-T-tri; (Δ) di-C^{21}-con-T-tri; (●) con-T-tri + 20 mM Ca^{2+}; (■) di-C^0-con-T-tri + 20 mM Ca^{2+}; (▲) di-C^{21}-con-T-tri + 20 mM Ca^{2+}.

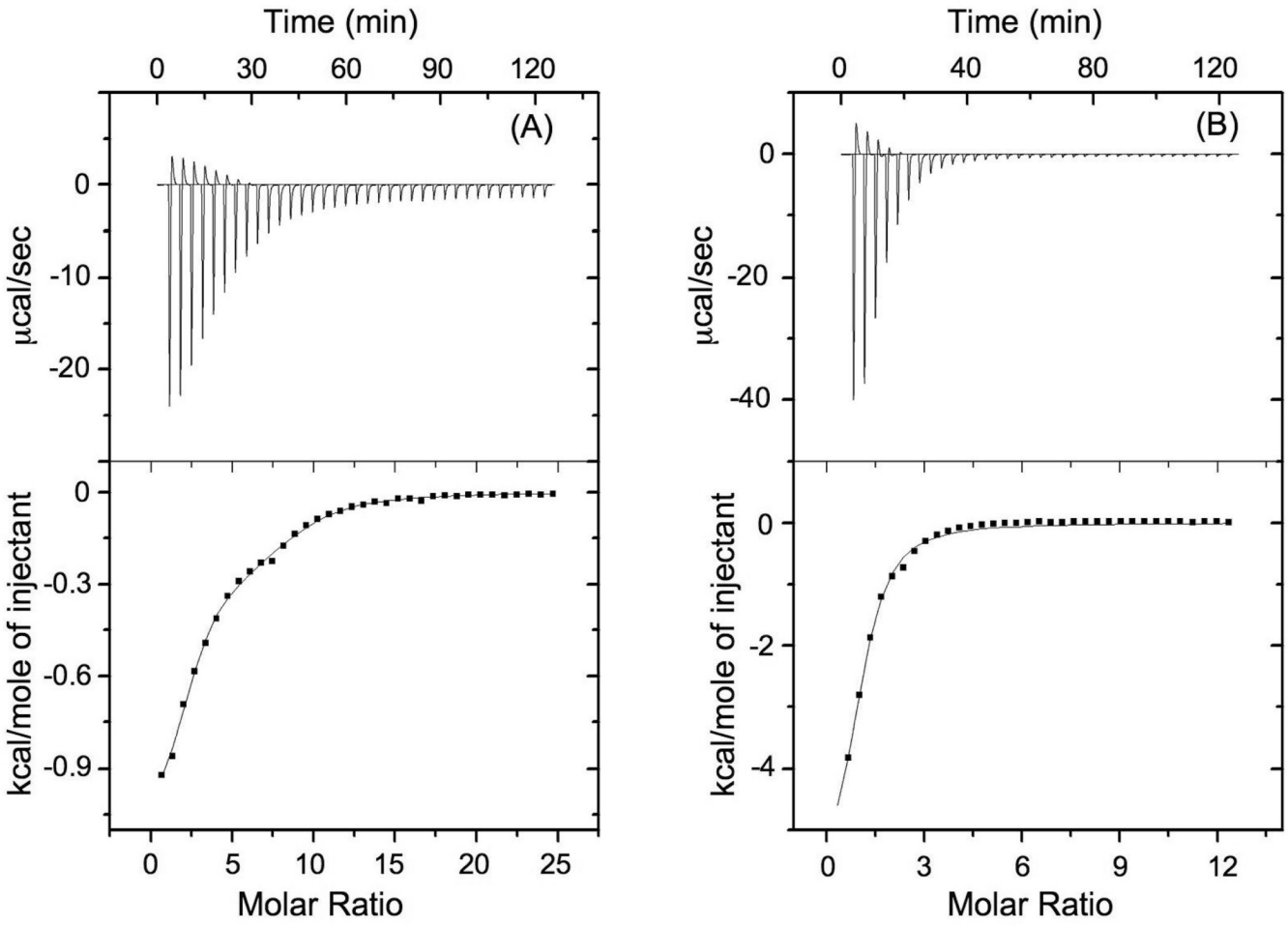

Fig. 3.

Calorimetrically-monitored data of the raw heat changes (upper panels) and integrated heats and calculated fits (bottom panels) for the titration of con-T-tri with 100 mM $CaCl_2$ or 50 mM $MgCl_2$. The metal ion stoichiometries and binding constants derived from these data are summarized in Table 1. A, con-T-tri/Ca^{2+}; B, con-T-tri/Mg^{2+}.

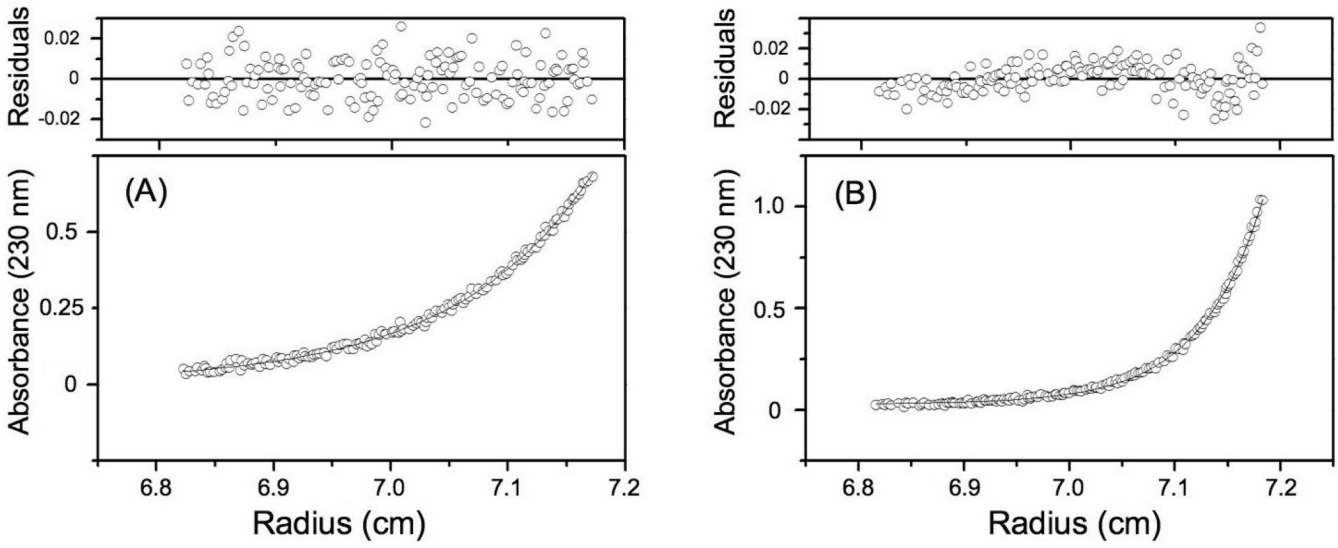

Fig. 4.

Sedimentation equilibrium scans and fits (bottom panels) for the MW_{app} of con-T-tri at 20 °C in the absence and presence of 20 mM $CaCl_2$. The data were fitted to the model for a single ideal species. Residuals for the displayed fits are shown in the upper panels. The values for MW_{app} derived from these data are included in Table 1. A, con-T-tri; B, con-T-tri + Ca^{2+}.

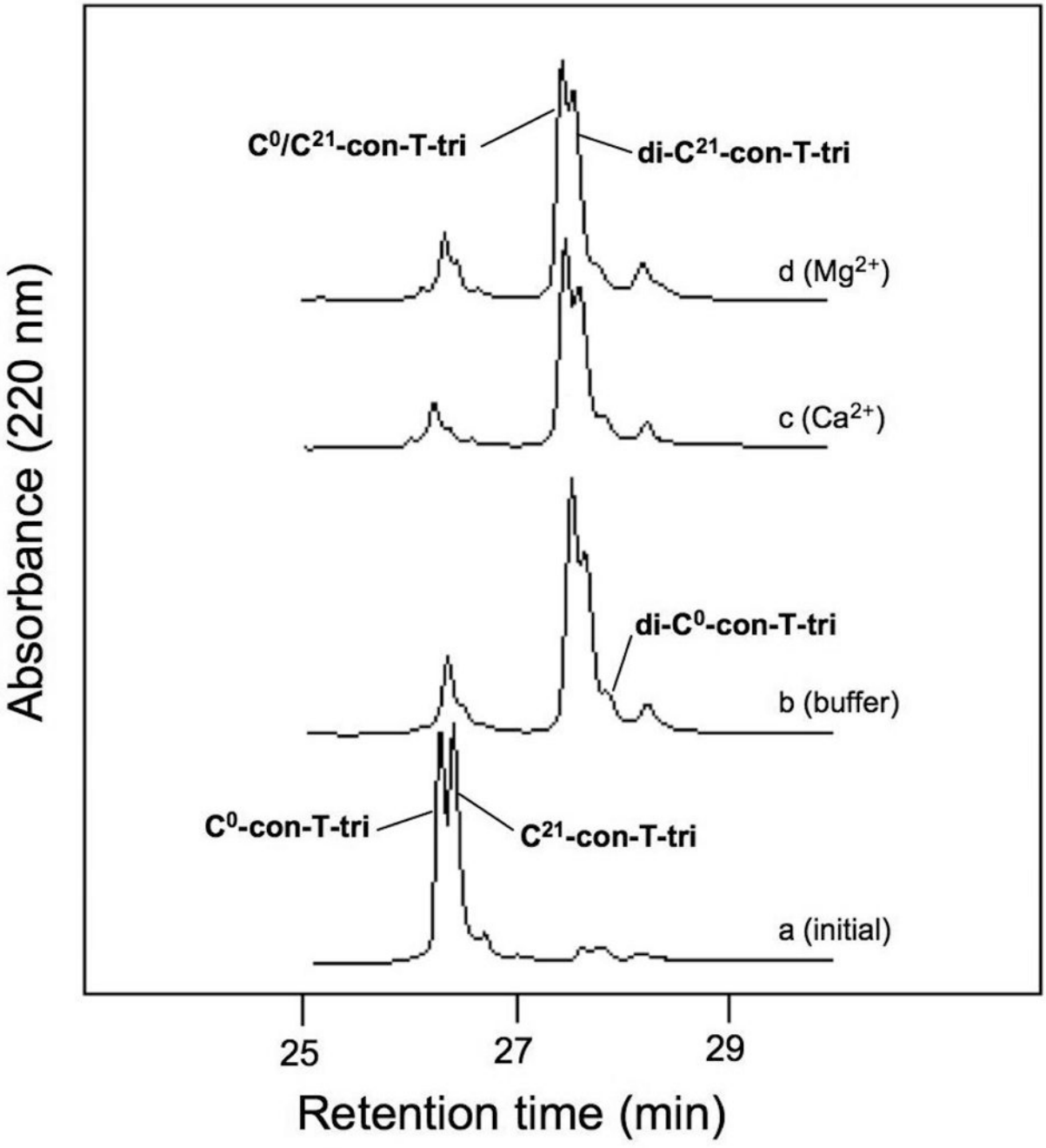

Fig. 5.

HPLC analyses of the equilibrium distribution of oxidation products following the incubation of C^0-con-T-tri and C^{21}-con-T-tri in the absence (b) or presence of 20 mM $CaCl_2$ (c) or 20 mM $MgCl_2$ (d). The folding buffer was 50 mM sodium borate /100mM NaCl, pH 8.2. Chromatograms were obtained as described in “Materials and methods”.

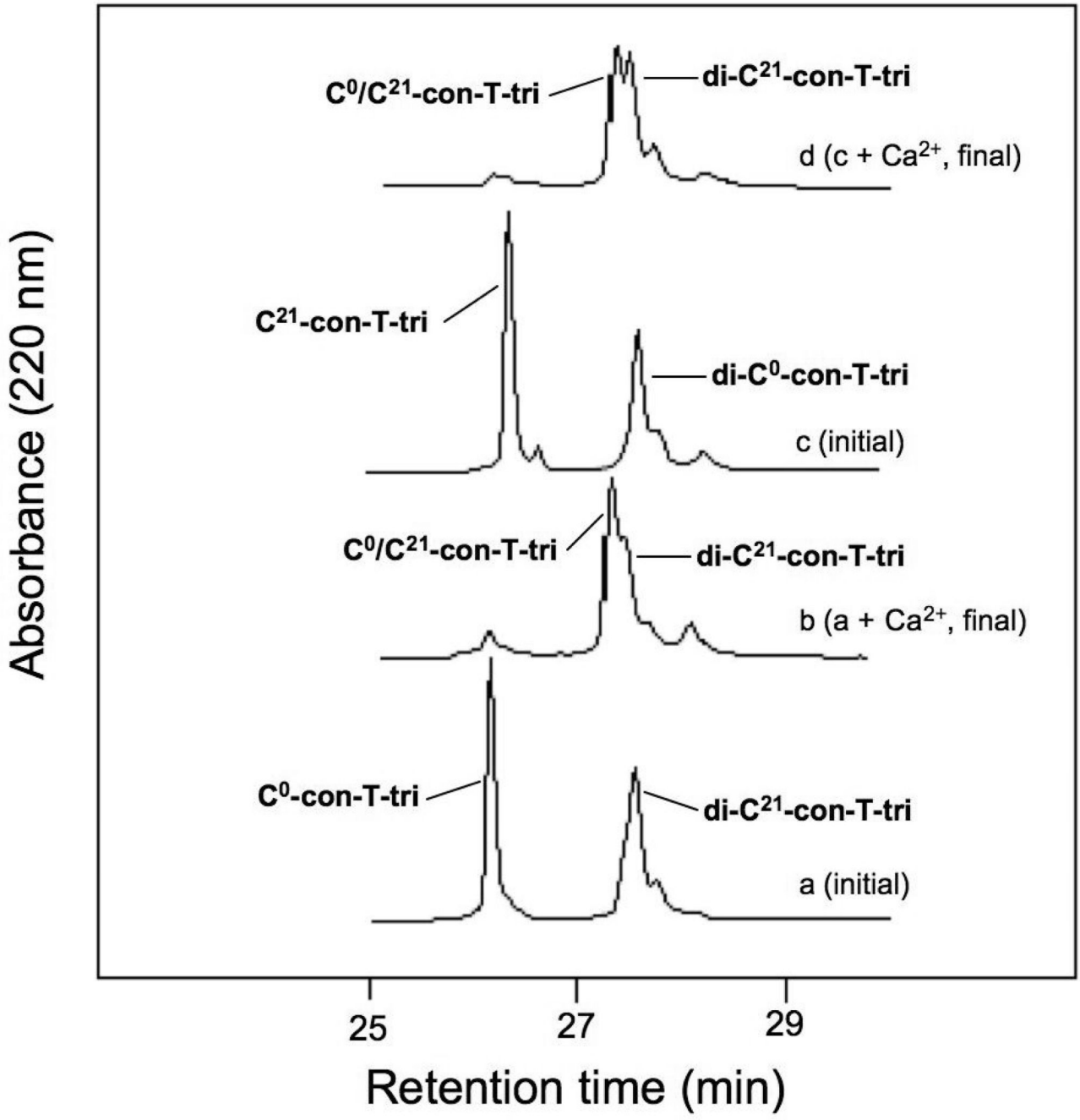

Fig. 6.

HPLC-monitored thiol-disulfide exchange assays of reduced momomeric and homostranded disulfide-linked variants of con-T-tri. The equilibrium distribution of oxidation products was assessed following the incubation of C^0-con-T-tri and di-C^{21}-con-T-tri (a, b) and the incubation of C^{21}-con-T-tri and di-C^0-con-T-tri (c, d). The folding buffer was 50 mM sodium borate/ 100mM NaCl, pH 8.2. $CaCl_2$ was present at a concentration of 20 mM. Chromatograms were obtained as described in “Materials and methods”.

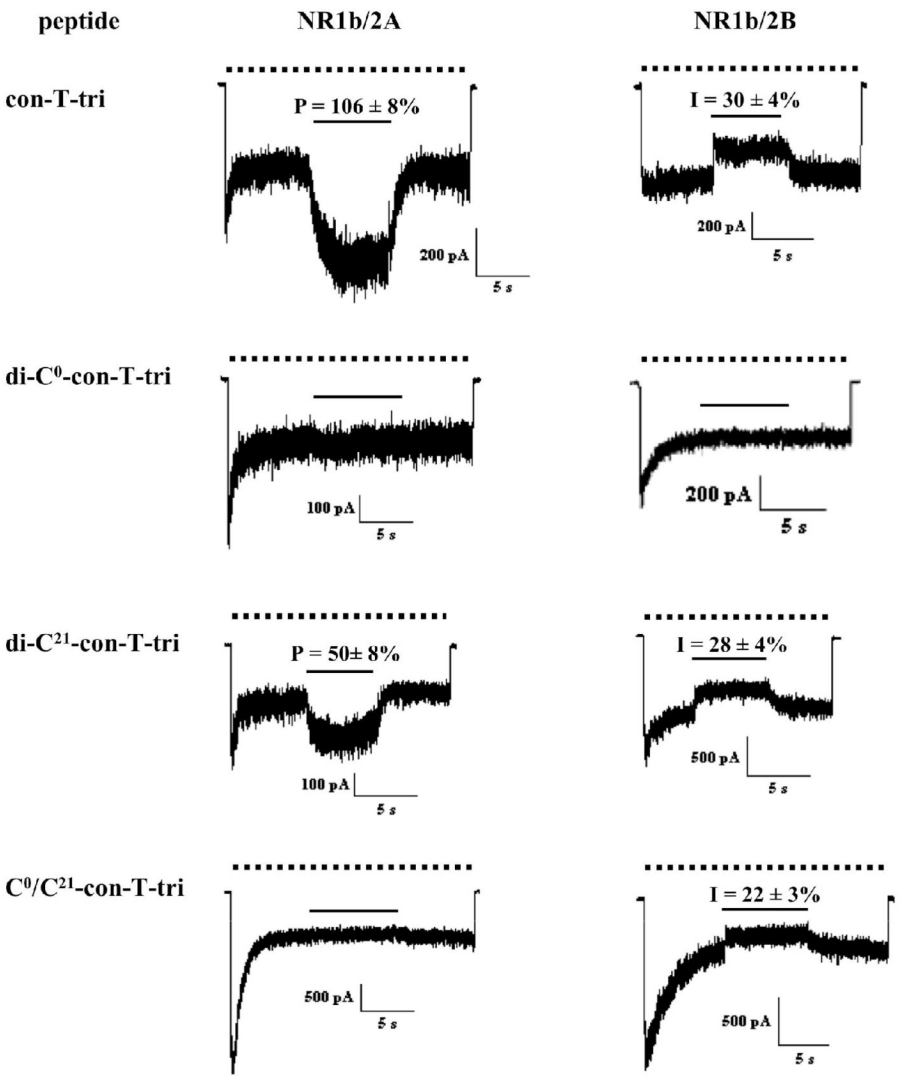

Fig. 7.

Representative time-course data of the effects of con-T-tri and disulfide-linked derivatives thereof on NMDA-elicited currents in HEK293 cells expressing NR1b/2A (*left* column) and NR1b/2B (*right* column) combinations of NMDA receptor subunits. Current was elicited by the application of 100 μM, 10 glycine μM (dotted line) followed by application of the designated peptide at a concentration of 40 μM (solid line). The percent inhibition (I) or potentiation (P) of the steady-state current (± S.D.) is indicated above each peptide application bar and represents the average of 4–7 cells tested at the indicated NMDA receptor subunit combination.

Table 1

Properties of metal-ion associated con-T-tri and con-T[K7γ].

Peptide	Metal ion[a]	% helix	MW_{app}[b]	f_{di}[c]	*n*[d]	K_d[d](μM)
con-T-tri	none	5	3320 ± 300	0		
	Ca^{2+}	63	6490 ± 450	0.76	2.2	26
					6.4	345
	Mg^{2+}	67	3460 ± 190	0.03	1.0	126
con-T[K7γ][e]	none	12	3390 ± 290	0		
	Ca^{2+}	67	6660 ± 410	0.78	2.8	120
	Mg^{2+}	74	3330 ± 180	0	1.6	18
di-C^0-con-T-tri	none	6	5610 ± 290	0	n.d.	n.d.
	Ca^{2+}	58	10360 ± 210	0.66[f]	n.d.	n.d.
	Mg^{2}	67	6070 ± 330	0.07[f]	n.d.	n.d.
di-C^{21}-con-T-tri	none	33	5140 ± 190	0	n.d.	n.d.
	Ca^{2+}	36	5930 ± 230	0.03[f]	n.d.	n.d.
	Mg^{2}	35	n.d.[g]	n.d.	n.d.	n.d.
C^0/C^{21}-con-T-tri	none	38	5350 ± 200	0	n.d.	n.d.
	Ca^{2+}	40	6670 ± 230	0.11[f]	n.d.	n.d.
	Mg^{2}	41	n.d.	n.d.	n.d.	n.d.

[a] For both CD and analytical ultracentrifugation experiments, Ca^{2+} and Mg^{2+} concentrations of 20 mM (chloride salts) were employed.

[b] Values for MW_{app} were derived from 2 or 3 separate sedimentation equilibrium analyses. Data were fit to multiple scans acquired at speeds of 45,000 and 52,000 rpm.

[c] Fractional dimer content was calculated as previously described [9].

[d] Values for *n* (stoichimetry of metal ion binding) and K_d were determined by ITC as indicated in “Materials and Methods”.

[e] The presented values for con-T[K7γ] were excerpted from a previous study [10].

[f] Fractional dimer content was calculated by assuming that the stoichiometries of metal ion binding to the disulfide linked peptides are twice the values obtained from the ITC-derived stoichiometries for metal ion binding to con-T-tri.

[g] Not determined.